Study of the Mach-Zehnder Interferometric Technique for Dielectric Resonator Tuning

Héctor J. De Los Santos,[1] Christian Rusch,[2] Yi Chen[3]

[1]NanoMEMS Research, LLC, Irvine, CA 92604
[2]Institut für Hochfrequenztechnik und Elektronik, Karlsruher Institut für Technologie, Karlsruhe 76131, Germany
[3]Chair for Wireless Communications, Christian-Albrechts-Universität zu Kiel, Kiel 24143 Germany

Received 22 October 2012; accepted 25 February 2013

ABSTRACT: The modulation of a microwave-scale Mach-Zehnder interferometer coupled to a dielectric resonator (DR) tunes the DR resonance frequency. We report on a theoretical study to develop an understanding of the intrinsic tuning properties of an Mach-Zehnder interferometer ring-DR-microstrip line system and present an experimental verification. © 2013 Wiley Periodicals, Inc. Int J RF and Microwave CAE 00:000–000, 2013.

Keywords: dielectric resonator; tuning; satellite communications; Mach-Zehnder interferometer

I. INTRODUCTION

Rings and ring-based components, such as, resonators and filters, have been extensively studied [1–4]. Little work has been done, however, on applying rings as agents to effect the tuning of dielectric resonators (DR) [5]. In this novel context, it is conceptually profitable to think of the ring as operating as a Mach-Zehnder interferometer (MZI) and to explore how, when coupled to a DR, modulation of one of the MZI paths causes tuning of the DR. This approach is believed to be important because it paves the way to high-Q-preserving DR tuning. This article presents an extended version of a conference article [6], where a theoretical study, and experimental verification, of the intrinsic tuning properties of a metallic microwave-scale MZI-DR-transmission line system, of the type employed in, e.g., DR oscillators, was first presented. Section II presents an overview of the MZI ring and motivates its utilization as a tuning agent for DRs. Section III introduces the MZI-DR-microstrip line system, develops an understanding of its operation, a circuit model, and presents the experimental verification of DR tuning using this scheme.

Correspondence to: H. De Los Santos; e-mail: hjd@nanomems-research

DOI: 10.1002/mmce.20753
Published online in Wiley Online Library (wileyonlinelibrary.com).

II. MZI-BASED TUNING CONCEPT

A. Overview of the MZI

The MZI, in its implementation as a metallic microstrip ring, is depicted in Figure 1. It consists of two parallel curved paths, $i = 1,2$, forming an annular ring, characterized by propagation constant, $k_i = \omega\sqrt{L_{r_i}C_{r_i}}$, where ω is the wave frequency and L_r and C_r, the inductance and capacitance per unit length, respectively. When the propagation constants are equal, the input wave, after being split at the input junction, propagates down both paths and is recreated at the output junction, where recombination occurs. On the other hand, causing the propagation constants of the two ring paths to be unequal results in wave amplitude at the output that exhibits a degree of interference. Assuming unit input wave amplitude and equal splitting in both ring arms, Figure 1, the output wave amplitude is $t = e^{ik_1L}/\sqrt{2} + e^{ik_2L}/\sqrt{2}$. Then, the interference behavior is mathematically captured by the transmission coefficient of the structure, namely:

$$T = |t|^2 = 1 + \cos[L \cdot (k_2 - k_1)], \tag{1}$$

where L is half the ring mean circumference. Clearly, the maximum of T is obtained whenever the cosine argument equals zero or an integer multiple of 2π. Now, if the MZI ring had no outgoing transmission line, it is easy to see that there could be no transmission, and, therefore, the waves on each ring arm would counter propagate, establishing a standing wave pattern in the ring. Under these

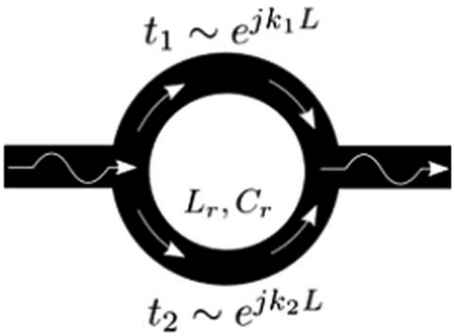

Figure 1 Sketch of MZI.

circumstances, it is well known that a resonance condition exists, whose frequency is well approximated by:

$$f_n = \frac{nc}{2L\sqrt{\varepsilon_{\text{eff}}(f)}}, \tag{2}$$

where $n = 1, 2, \ldots$, is the mode number, c is the speed of light in vacuum, and $\varepsilon_{\text{eff}}(f)$ is the frequency-dependent relative dielectric constant of the substrate supporting the ring.

B. MZI Ring Tuning

To study the intrinsic tuning properties of the tunable ring, the structure shown in Figure 2 is considered.

It may be construed as consisting of an asymmetric ring made up of the parallel connection of one microstrip transmission line (TL) of length L_4 and width w, and another TL consisting of the tandem connection of three TL segments of length and widths (L_1,w), (L_2,w_2), and (L_3,w), respectively. Other asymmetric MZI ring parameters are its mean radius, r, and the mean circumference $2L = 2\pi r = L_1 + L_2 + L_3 + L_4$, with:

$$L_1 = r\left(\pi - \left[\frac{\theta}{2} + \phi\right]\right), \tag{3}$$

$$L_2 = r\theta, \tag{4}$$

$$L_3 = r\left(\phi - \frac{\theta}{2}\right), \tag{5}$$

$$L_4 = r\pi. \tag{6}$$

For a given mean ring circumference, $2L$, tuning is effected by changing (L_2,w_2). This segment is positioned at the azimuthal angle ϕ and has an angular extent θ, Figure 2.

In addition, at a frequency f, the electrical parameters of the ring are given by the propagation constant of each TL segment j, $\gamma_j = \alpha_j + i\beta_j = \alpha_j + ifn_j$, where α_j and β_j are the attenuation and phase constants in segment j, with $\beta_j = 2\pi f\sqrt{\mu_0\varepsilon_0\varepsilon_{\text{eff}_j}} = fn_j$, and μ_0 and ε_0 are the vacuum permeability and permittivity, respectively. The intrinsic tuning properties of the asymmetric ring are obtained by conceptually assuming it to be a two-port network, driven at its input and output ports by voltages and currents v_1, i_1 and v_2, i_2, respectively, Figure 2. The ring's return loss, $S_{R\_11} = S_{R\_11\_N}/S_{R\_D}$, and transmission, $S_{R\_21} = S_{R\_21\_N}/S_{R\_D}$, were obtained analytically in terms of the overall ring admittance parameters (Y_{R_ij}), by computing the ABCD parameters of the two paths, converting the parameters of each path to admittance parameters, and adding the resulting Y-parameters of each path. The S-parameter expressions are long, so their numerators, $S_{R\_11\_N}$ and $S_{R\_21\_N}$, and their common denominator, S_{R_D} are given separately in Eq. (7a), where Z_0 is the reference impedance and the attenuation (α) has been taken as zero. The S-parameters, computed with Eq. (7a), are plotted in Figure 3a; the transmission follows the same behavior of the symmetric ring [Eq. (1)]. There are no closed-form expressions for the resonance frequencies of the asymmetric MZI ring, since they derive from the transcendental equation obtained from seeking the roots of Eq. (7c) [shown as "from Eq. 7c" in Fig. 3c]; however, in a design, Eq. (2) is a good starting point.

The formulas are verified by comparing their predicted tuning frequencies, given by the minimum of S_{R_11} as computed from Eq. (7a), with the frequency of the minima obtained from CST [7] simulations, Figure 3b; the "kink" at $\theta = 14°$ is predicted by Eq. (7a) and is due to the increased proximity to the main resonance of a higher-frequency resonance as θ approaches 14°. As clearly seen in Figure 3c, increasing the tuning sector length, θ, causes the resonance frequency to decrease, as should correspond to adding the tuning sector capacitance. It must be mentioned also that, given the nonlinear dependence of Eq. (7a) on ϕ (through L_1 and L_3), the tuning range is a function of the azimuthal angle ϕ.

C. MZI Ring Coupling to Transmission Line

While the properties of ring-TL coupling have been studied [3,4], studies on the effect that ring tuning, as revealed

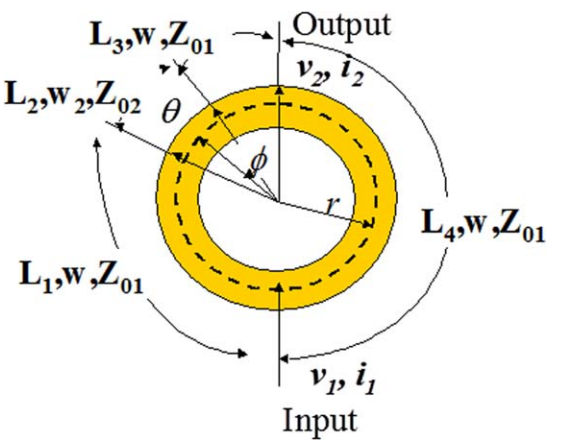

Figure 2 Description of asymmetric microstrip MZI ring: θ, tuning sector; ϕ, azimuthal position of tuning sector; r, mean radius; w, unloaded ring width; w_2, tuning sector (loaded) ring width; Z_{01}, Z_{02}, characteristic impedances of indicated segments. [Color figure can be viewed in the online issue, which is available at wileyonlinelibrary.com.]

here, produces on TL properties are lacking. Simulations in CST, Figure 3d, exhibit a minimum in the transmission, whose frequency decreases with increase in tuning sector angle, θ. This suggests a way of tuning the transmission of the microstrip line and, as shown next, may be exploited to tune a DR.

III. MZI-BASED DIELECTRIC RESONATOR TUNING CONCEPT AND EXPERIMENTAL VERIFICATION

A. Fundamental Concept

The idea of applying the tuned MZI ring to effect DR tuning derives from extending the DR-microstrip model [8], Figure 4, to the DR-MZI ring, Figure 5, except that in the latter case the transformer coupling N_t becomes variable, reflecting MZI tuning. Specifically, the magnetic field (even mode) microstrip-DR coupling, captured by N_t, and obtained by Komatsu and Murakami [8] as:

$$N_t^2 = 4\omega\left(\int_0^l \left(\frac{M(x)}{\sqrt{L_0}}\right)\cos(kx)dx\right)^2, \tag{7}$$

may be made variable by tuning the propagation constant of the microstrip, k.

$$\begin{aligned} S_{R\_11\_N} = {} & 0.5\csc[fL_4n_1]\left(-8Z_0^2Z_{01}Z_{02}+2Z_{01}Z_{02}\left(Z_{01}^2\cos[f(L_1+L_3-L_4)n_1]+(4Z_0^2-Z_{01}^2)\cos[f(L_1+L_3+L_4)n_1]\right)\cos[fL_2n_2]\right) \\ & -\left(Z_{01}\left(-2iZ_0(Z_{01}-Z_{02})(Z_{01}+Z_{02})\cos[f(L_1-L_3-L_4)n_1]+2iZ_0(Z_{01}-Z_{02})(Z_{01}+Z_{02})\cos[f(L_1-L_3+L_4)n_1]\right.\right. \\ & +Z_{01}(-Z_{01}^2+Z_{02}^2)\sin[f(L_1-L_3-L_4)n_1]+Z_{01}(Z_{01}^2+Z_{02}^2)\sin[f(L_1+L_3-L_4)n_1]+Z_{01}(Z_{01}-Z_{02})(Z_{01}+Z_{02})\sin \\ & \left.\left.[f(L_1-L_3+L_4)n_1]+(4Z_0^2-Z_{01}^2)(Z_{01}^2+Z_{02}^2)\sin[f(L_1+L_3+L_4)n_1]\sin[fL_2n_2]\right)\right) \end{aligned} \tag{7a}$$

$$S_{R\_21\_N} = -4iZ_0Z_{01}\left(Z_{01}Z_{02}+\csc[fL_4n_1]\left(Z_{01}Z_{02}\cos[fL_2n_2]\sin[f(L_1+L_3)n_1]+(Z_{02}^2\cos[fL_1n_1]\cos[fL_3n_1]-Z_{01}^2\sin[fL_1n_1]\sin[fL_3n_1])\sin[fL_2n_2]\right)\right) \tag{7b}$$

$$\begin{aligned} S_{R\_D} = {} & Z_{01}Z_{02}\csc[fL_4n_1]\left(4Z_0^2+\cos[fL_2n_2]\left(Z_{01}^2\cos[f(L_1+L_3-L_4)n_1]-(4Z_0^2+Z_{01}^2)\cos[f(L_1+L_3+L_4)n_1]-4iZ_0Z_{01}\sin[f(L_1+L_3+L_4)n_1]\right)\right) \\ & +2\left(\cos[fL_3n_1]\left(\cos[fL_1n_1]\left(Z_0^2Z_{01}^2+(Z_0^2+Z_{01}^2)Z_{02}^2-2iZ_0Z_{01}Z_{01}^2\cot[fL_4n_1]+Z_0(Z_{01}^2+Z_{02}^2)(iZ_{01}+Z_0\cot[fL_4n_1])\sin[fL_1n_1]\right)\right.\right. \\ & \left.\left.+\left(Z_0(Z_{01}^2+Z_{02}^2)\cos[fL_1n_1](iZ_{01}+Z_0\cot[fL_4n_1])-\left(Z_{01}^4+Z_0^2(Z_{01}^2+Z_{02}^2)-2iZ_0Z_{01}^3\cot[fL_4n_1]\right)\sin[fL_1n_1]\right)\sin[fL_3n_1]\right)\sin[fL_2n_2]\right] \end{aligned} \tag{7c}$$

In particular, if we consider the MZI ring-DR structure, shown in Figure 5, then it is clear that, in the immediate vicinity of the coupling region, over a certain extent of microstrip of length $2l$, the MZI ring may be approximated by a microstrip of characteristic impedance Z_0 and propagation constant k. In this context, this structure may also be modeled in a similar fashion to the DR-microstrip of Figure 4, except that, due to the tuning produced by the loaded sector, see Figure 2, k becomes variable and so does N_t. One concludes that a structure capable of tuning the frequency properties of a DR may be realized by configuring an MZI ring-DR-microstrip structure [9].

B. Basic MZI Ring-DR-Microstrip Structure

The basic MZI ring-DR-microstrip structure is depicted in Figure 6a. In it, the input microstrip power couples via the magnetic field (even mode) to the DR, Figure 6b, and from the DR to the MZI ring, where a standing wave is established, Figures 6b and 6c.

While the DR size is dictated by the frequency of interest, f_0, and may be determined from available software, e.g., from Transtech, Inc. [10], the selection of the MZI Ring size is nontrivial [5]. On the one hand, since, as discussed by Lu and Ferendeci [3,4], coupling to the ring occurs via both odd (electric field coupling) and even (magnetic field coupling) modes, care must be exercised in choosing its size such that the resonance frequency for one of the ring's even modes coincides with that of the DRs (i.e., f_0). On the other hand, obtaining maximum overall quality factor requires minimizing the MZI ring's radiated power [5]. Through studies of the ring's radiation efficiency, under the conditions that it both exhibited an even mode coupling and reduced radiation efficiency at f_0, we determined that the MZI ring circumference should be chosen so the frequency of its second resonance mode (which is an even mode) coincided with f_0. For DR operation at $f_0 \sim 10.2$ GHz, we determined that an MZI ring with mean radius of 7.45 mm was adequate [5].

C. Tunable MZI Ring-DR-Microstrip Structure

Tuning of the DR, as discussed in Section II.B, is effected by varying the angular extent, θ, of a sector centered at

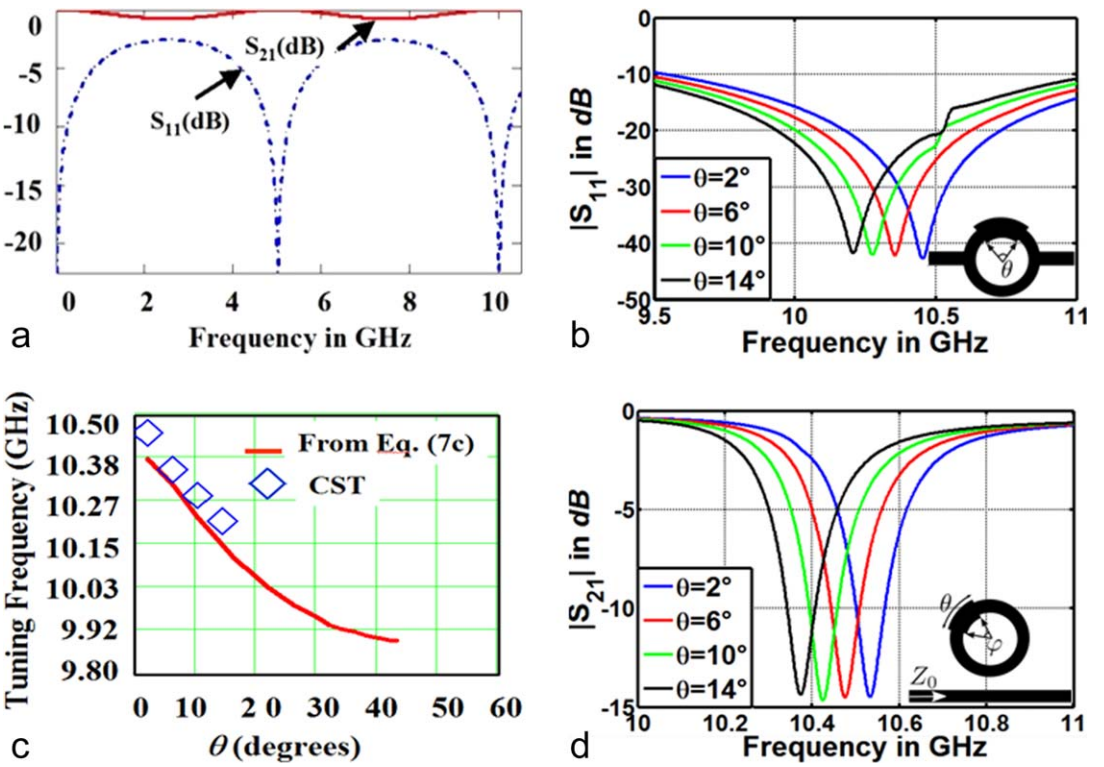

Figure 3 (a) S-parameters of asymmetric MZI ring at $\phi = 90°$, $\theta = 4°$. (b) Insertion loss of CST-simulated loaded MZI ring (sketch in inset), with $\phi = 90°$, for various tuning sector angles. (c) Tuning frequency versus tuning sector angle for MZI ring in Figure 3b. MZI ring parameters: mean ring diameter, 6.95 mm; ring trace width, 0.5 mm; substrate thickness and relative permittivity, 0.635 mm and 10.2, respectively; metallization thickness, 0.017 mm. (d) CST-computed microstrip transmission (S_{21}) versus frequency with tuned-sector angle, θ, as a parameter, and $\phi = 135°$. The tuned sector width is 1 mm. [Color figure can be viewed in the online issue, which is available at wileyonlinelibrary.com.]

an azimuth angle ϕ, on the ring, Figure 7. As surmised from CST simulations of the structure, Figure 7, changes in sector length cause the magnetic field standing wave to rotate.

The effect of this rotation is to reduce the magnetic field that couples the MZI ring and DR, see Figure 8b.

The resulting DR tuning, manifested in the microstrip transmission (S_{21}), Figure 8c, is due to the concomitant change in N_t and is explained by the MZI ring-DR-

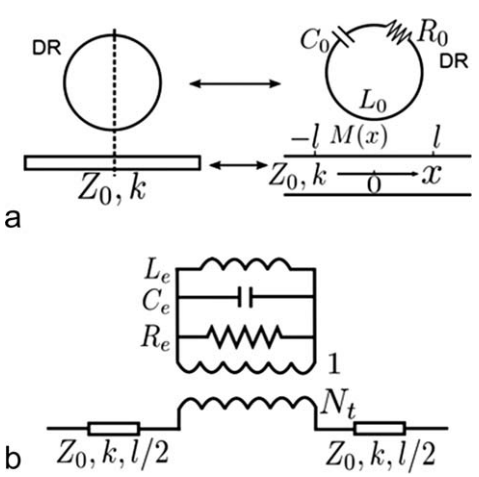

Figure 4 (a) Distributed DR-microstrip model; (b) lumped DR-microstrip circuit model. [Color figure can be viewed in the online issue, which is available at wileyonlinelibrary.com.]

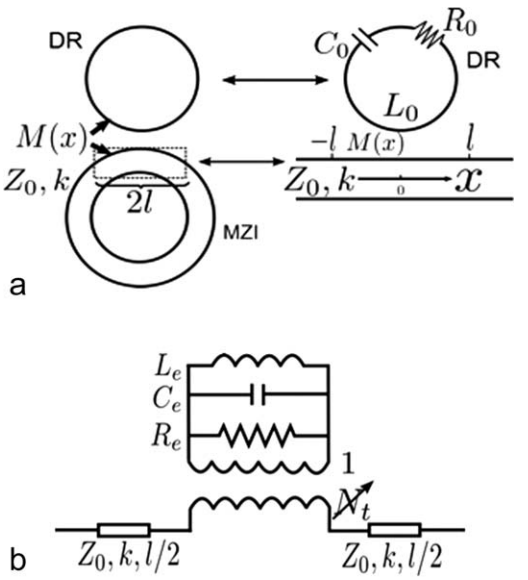

Figure 5 (a) DR-MZI ring distributed model; (b) lumped DR-MZI ring circuit model. [Color figure can be viewed in the online issue, which is available at wileyonlinelibrary.com.]

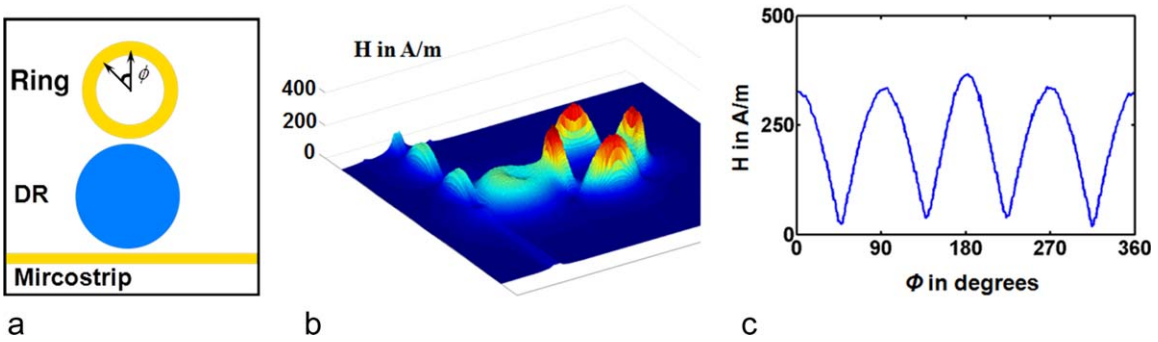

Figure 6 (a) MZI ring-DR-microstrip structure; (b) magnetic field in the structure; (c) magnetic field under the MZI ring along its mean radius, computed with CST. The structure has the parameters given in the caption of Figure 3, and the DR has a nominal Q of 5000. [Color figure can be viewed in the online issue, which is available at wileyonlinelibrary.com.]

microstrip circuit model, Figure 9. To extract this model, we began with the circuit model for the DR-microstrip, obtained with software by Transtech, Inc. [9].

Then, these initial RLC-transformer-microstrip circuit parameters were optimized so its transmission (S_{21}) would match the structures' CST-computed S_{21}, particularly, in the neighborhood of the resonance frequency. Next, the RLC elements for the MZI ring were computed from analytical formulas [1,2,11–13]. Fixing these set of parameters, the overall MZI ring-DR-microstrip S_{21}, computed with CST [7] at various frequencies, were matched at each frequency in ADS [14] with the model in Figure 9a by using the turns ratio N_t as the *single* adjustable parameter. Comparisons of the circuit model results computed in ADS and the full-wave results computed in CST are shown in Figures 9b and 9c, respectively. As can be seen, the circuit model fits very well the full-wave CST simulations. Therefore, tuning is caused by variation in tuning sector length, which causes rotation of the magnetic field standing wave on the ring, which causes the magnitude of the field between the DR and MZI ring to change, which causes N_t to change and, consequently, causes the MZI ring's impedance load "seen" by the DR to change, ultimately tuning it.

D. Deformed MZI Ring and Experimental Verification

As discussed above, the DR resonance frequency can be tuned by varying the sector length, θ, of the MZI ring coupled to it. However, in addition to frequency tuning range, our interest included elucidating how to obtain a concomitantly large Q [5]. Our investigations toward that goal concluded that the circular MZI ring is capable of effecting DR tuning while maintaining a relatively high Q, but it exhibits a trade-off between them [5]. For example, for a target $f_0 \sim 10$ GHz and a nominal DR Q of 5000, we found that a tuning sector centered at $\phi = 30°$, exhibited a maximum Q of 663 and a tuning range of 58 MHz, but for $\phi = 90°$, the maximum Q was 923 and the tuning range was 20 MHz. The pursuit of improving this Q-tuning range trade-off, detailed in [5], led us to conceive of, and adopt, a configuration that would increase the MZI ring-DR-microstrip coupling, namely, the deformed ring structure [5], Figures 10a and 10b.

Theoretically, for the $\phi = 30°$ case (the $\phi = 90°$ case has no counterpart in the deformed ring structure), the deformed ring structure resulted in a maximum Q of 956 and a tuning range of 50 MHz [5]. This Q represents a 44% increase over that exhibited by the corresponding circular-ring structure and a 16% decrease in tuning

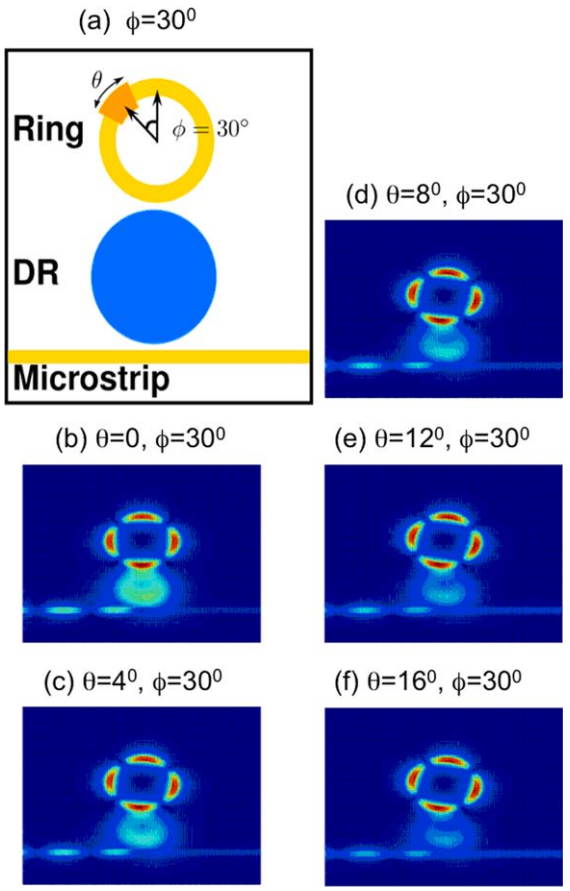

Figure 7 (a) Tunable MZI ring-DR-microstrip structure; right: (b)–(f) magnetic field under MZI ring at various tuning sector lengths θ The tuned-sector width is 1 mm. [Color figure can be viewed in the online issue, which is available at wileyonlinelibrary.com.]

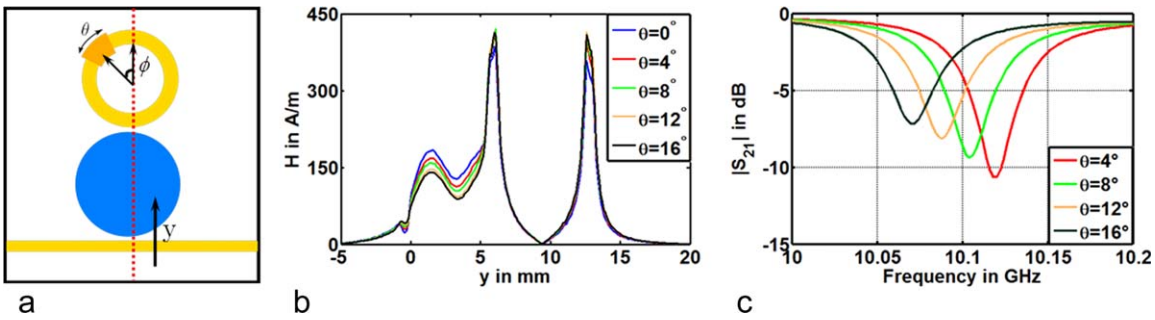

Figure 8 (a) MZI ring-DR-microstrip structure with tunable sector at $\phi = 45°$ showing line of symmetry y; (b) magnetic field along line of symmetry y at various sectorial lengths θ (c) S_{21} of structure in (a) showing tuning at various sectorial length θ. [Color figure can be viewed in the online issue, which is available at wileyonlinelibrary.com.]

bandwidth, for the same change in tuning-sector dimensions, suggesting a more favorable trade-off between Q and bandwidth for the deformed-sector ring [5]. Both the circular ring and the deformed ring structures were fabricated and tested; however, due to its superiority [5], we present here the results of the deformed ring-based structure, Figures 10a–10c. In particular, the variation in tuning sector angles was realized by fabricating three separate structures, like Figure 10c, each with $\theta = 2°$, 6°, or 10°. Defining the tuning sector this way in the study provided a controlled way (i.e., one that is reproducible by others) of varying its size, which otherwise could be done by, e.g., manually placing on the ring gold ribbons of varying sizes, as is customary practice when "tuning" microwave integrated (i.e., alumina-based, etc.) circuits. The measured and CST-simulated S_{21} and S_{11} for these structures, shown in Figures 10d and 10e, exhibit a tuning range of ~32 MHz about $f_0 \sim 9.8$ GHz and a Q factor between 983 and 1089, for sector angles $\theta = 2°$, 6°, 10°, thus verifying the DR tuning concept. Implemented this way, DR-based circuits may be "manually" fine-tuned to a precise frequency. On the other hand, we envision *in future work* implementing DR tunability without manual intervention, e.g., through voltage control, by exploiting microelectromechanical systems/nanoelectromechanical systems fabrication technology [9]. While there is a discrepancy

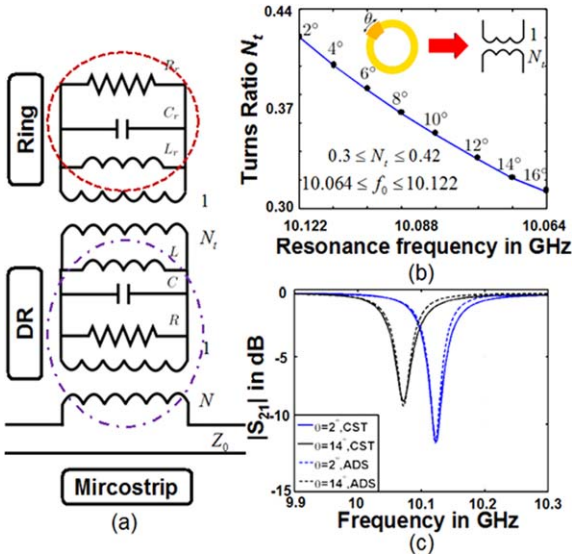

Figure 9 (a) MZI ring-DR-microstrip circuit model; (b) Variation of turns ratio as a function of tuning frequency; (c) S_{21} plot comparing circuit model and CST simulation results. [Color figure can be viewed in the online issue, which is available at wileyonlinelibrary.com.]

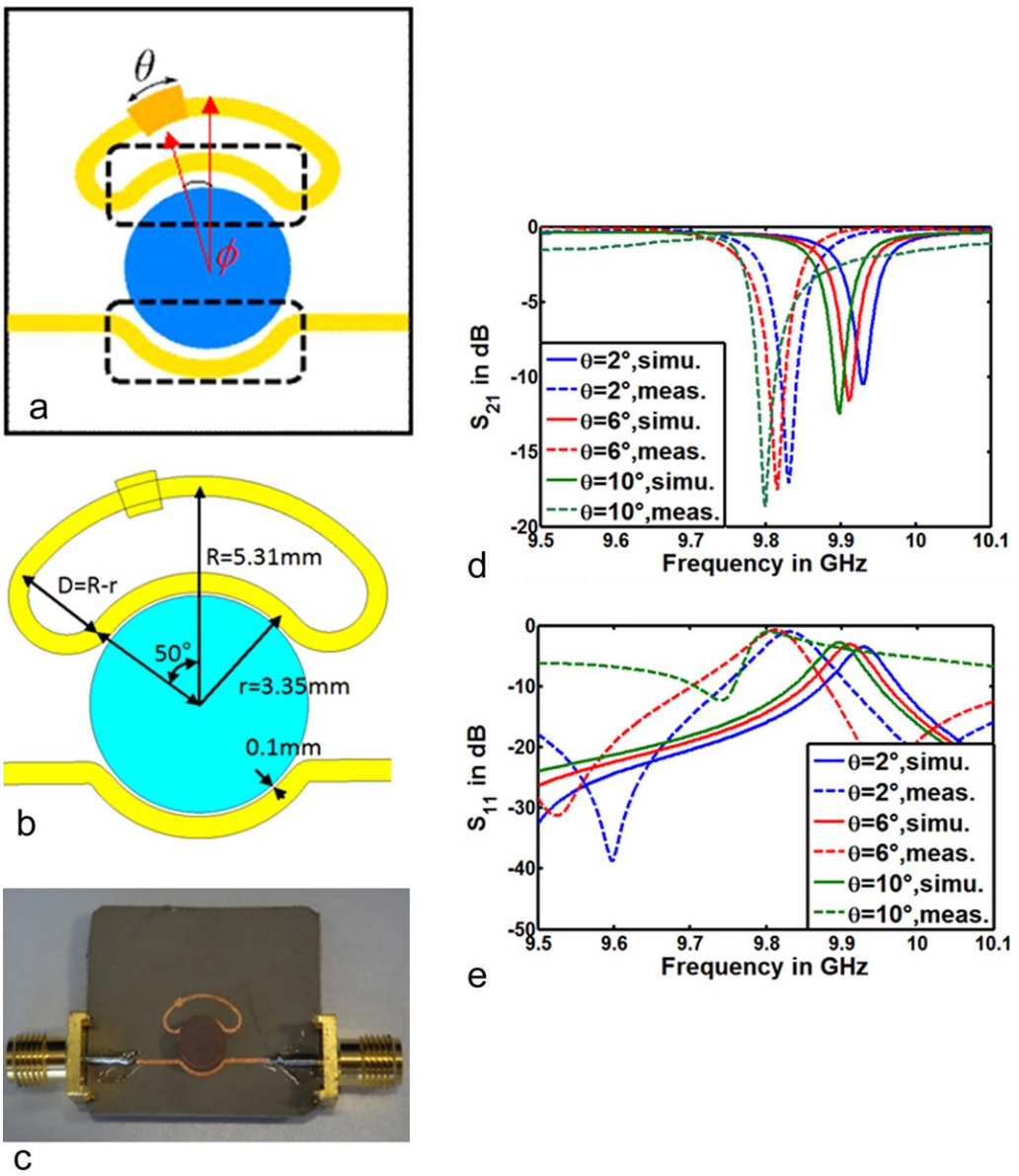

Figure 10 (a) Sketch of MZI ring-DR-microstrip structure (in practice, the indicated tuning sector may be implemented manually with a gold ribbon, until the desired resonance frequency is obtained); (b) details of pertinent deformed ring dimensions; (c) picture of typical fabricated MZI ring-DR-microstrip structure. Three structures with $\theta = 2°, 6°, 10°$ were fabricated; (d), (e) measured and CST-simulated S_{21} and S_{11} of fabricated structure shown in (c). Parameters: $\phi = 30°$; ring trace width, 0.5 mm; substrate thickness and relative permittivity, 0.635 mm and 10.2, respectively; metallization thickness, 0.017 mm; tuned-sector width, 1 mm; both the DR-microstrip and DR-ring separation distances were 0.1 mm; nominal DR Q was 4545 at 10 GHz and 5000 at 9.6 GHz, its diameter was 5.842 mm, its height, 2.7432 mm, and its relative permittivity 35.94. [Color figure can be viewed in the online issue, which is available at wileyonlinelibrary.com.]

between measured and CST-simulated center frequencies, probably due to the effects of the housing, the tuning behavior is very similar in both cases. This eliminates the possibility of tuning behavior due to reproducibility issues and does corroborate the verification of the concept.

IV. CONCLUSION

A theoretical study to develop an understanding of the modulation of a metallic microwave-scale MZI coupled to a DR to effect tuning of the latter's resonance frequency has been presented including an experimental verification of the concept. We have shown that the tuning range is related to the spatial overlap/coupling between MZI-ring and DR magnetic fields, which is varied when a tuning sector on the MZI ring causes the latter's magnetic field standing wave to rotate. The experimental verification showed a tuning range of 32 MHz about 9.8 GHz, together with a Q between 983 and 1089. In future work, the concept studied here will be implemented by exploiting microelectromechanical systems/nanoelectromechanical systems fabrication technology to create DR-based

microwave circuits, including oscillators and filters, which are tunable without manual intervention, e.g., through voltage control [9].

ACKNOWLEDGMENTS

This work was supported in part by a Deutsche Forschungsgemeinschaft (DFG) Mercator Visiting Professorship Award to H. J. De Los Santos. He gratefully acknowledges the hospitality of Professor Thomas Zwick, Head of the Institut für Hochfrequenztechnik und Elektronik (IHE), Karlsruher Institut für Technologie (KIT), during his stay at KIT. He also thanks Professor T. Zwick and Professor Werner Wiesbeck, both of IHE, KIT, for encouraging the submission of the research proposal that resulted in this DFG Mercator Gastprofessur award. The authors thank Transtech, Inc., for donation of the dielectric resonators used in the experiments.

REFERENCES

1. K. Chang and L.-H. Hsieh, Microwave ring circuits and related structures, John Wiley & Sons, New York, 2004.
2. K. Chang, Microwave ring and circuits and antennas, Wiley, New York, 1996.
3. S.-L. Lu and A. M. Ferendeci, Coupling modes of a ring resonator side coupled to a microstrip line, Electron Lett 30 (1994), 1314–1315.
4. S.-L. Lu and A. M. Ferendeci, Coupling parameters for a side-coupled ring resonator and a microstrip line, IEEE Trans Microwave Theory Tech, 44 (1996), 953–956.
5. H.J. De Los Santos, Y. Chen, and C. Rusch, Properties of metallic microwave-scale Mach-Zehnder interferometers for dielectric resonator tuning, Electron Letts, 47 (2011), 506–508.
6. H.J. De Los Santos, C. Rusch, and Y. Chen, Study of the Mach-Zehnder interferometric technique for dielectric resonator tuning, 2012 IEEE MTT-S Int. Microwave Symposium Digest (MTT).
7. CST Studio Suite 2010, Computer Simulation Technology, Inc.
8. Y. Komatsu and Y. Murakami, Coupling coefficient between microstrip line and dielectric resonator, IEEE Trans Microwave Theory Tech, 31 (1983), 34–40.
9. H. J. De Los Santos, Resonator tuning system, U.S. Patent No. US6.304.153.B1.
10. Transtech—Windows-based CAD and Transtech parts selector guides for dielectric resonators. Available at: http://www.sss-mag.com/swindex1.html#rf
11. J.R. Bray and L. Roy, Microwave characterization of a microstrip line using a two-port ring resonator with an improved lumped-element model, IEEE Trans Microwave Theory Tech, 51 (2003), 1540–1547.
12. L.-H. Hsieh and K. Chang, Equivalent lumped elements g, l, c, and unloaded q's of closed- and open-loop ring resonators, IEEE Trans Microwave Theory Tech, 50 (2002), 453–460.
13. R. Hopkins and C. Free, Equivalent circuit for the microstrip ring resonator suitable for broadband materials characterization, IET Microwaves Antennas Propagation, 2 (2008), 66–73.
14. Advanced Design System, Available at: http://www.home.agilent.com/agilent/download.jspx?nid=-34346.0&cc=US&lc=eng&pageMode=DL.

BIOGRAPHIES

Héctor J. De Los Santos received the Ph.D. degree in electrical engineering from Purdue University, West Lafayette, IN, in 1989. Prior to founding NanoMEMS Research, LLC, in 2002, he spent 2 years as a Principal Scientist at Coventor, Inc., Irvine, CA. From 1989 to 2000, he was with Hughes Space and Communications Company, Los Angeles, CA, where he served as Principal Investigator and the Director of the Future Enabling Technologies IR&D Program. There, he pursued research in RF MEMS, quantum functional and photonic bandgap devices and circuits. He is author of four books and holds over 20 U.S. and European patents. His research interests include theory, modeling, simulation, design, and applications of emerging electronic devices and systems. During the 2010–2011 academic year, he held a German Research Foundation (DFG) Mercator Visiting Professorship at the Institut für Hochfrequenztechnik und Elektronik, Karlsruher Institut für Technologie (KIT), Germany. He is an IEEE Fellow.

Christian Rusch received the Dipl.-Ing. (FH) and the M.Sc. degree from the University of Applied Science Mannheim, Germany, in 2009. In 2009, he joined the Institut für Hochfrequenztechnik und Elektronik (IHE), as a Research Associate and is currently working toward the Dr.-Ing. degree. His current research topics include the design of integrated millimeter-wave radar sensors, LTCC modules, and millimeter-wave packaging. He also has experience in designing MEMS and switching components at high frequencies.

Yi Chen was born in Ningbo, China, in 1982. He received the Dipl.-Ing. degree from the Institut für Hochfrequenztechnik und Elektronik (IHE), Karlsruher Institut für Technologie (KIT), Karlsruhe, Germany, in 2011. He is now a Research Associate at the Chair of Wireless Communications, Institute of Electrical and Information Engineering, Christian-Albrechts University, Kiel, Germany, pursuing his Dr.-Ing. degree. His research interests include MEMS, antenna design, high frequency technologies, and wireless communication.